Development of a VGG19-Batch Normalization-based Framework for Accurate Detection and Classification of Sickle Cell Anaemia

Arularasi P[1], Dr.B.Pushpa[2]

[1] *Research Scholar, Assistant Professor*
[2]*Department of computer and information science, Annamalai university, Chidambaram, India.*

KEYWORDS

VGG19-Batch Normalization; Sickle Cell Anemia; Automated Diagnosis; RBC Classification; Medical Image Processing.

ABSTRACT:

Introduction:In Sickle Cell Anemia (SCA), a genetic blood disorder, RBC distort into a sickle shape, impairing oxygen transport and leading to serious medical complications. Effective therapy and management for patients with SCA rely on its rapid and reliable detection.

Objectives: Existing diagnostic methods are often labour-intensive, manual, and subject to variation due to personal interpretations by healthcare professionals. Automated diagnostic systems face challenges such as inefficient feature extraction and classification, inconsistent blood smear quality, and a lack of available datasets.

Methods: This paper proposes a deep learning framework based on VGG19 with Batch Normalization (VGG19-BN) to address these challenges in the identification and classification of SCA. The methodology includes pre-processing the images to enhance quality and standardize input data. BN layers are integrated into the VGG19 framework to stabilize training, reduce overfitting, and accelerate convergence. The convolutional layer's extract features to classify RBC into normal and sickle categories. The framework was trained and validated using high-quality blood smear images. The primary objective of this work is to develop a reliable and efficient diagnostic tool capable of achieving high accuracy while remaining user-friendly and interpretable in clinical settings.

Results: The results showed that the VGG19-BN model outperformed baseline deep learning systems and traditional techniques, achieving 96.7% accuracy in classification, 95.3% sensitivity, and 97.8% precision.

Conclusions:By improving both accuracy and efficiency, incorporating this method into clinical workflows could revolutionize SCA diagnosis and improve patient outcomes.

1. Introduction

SCA is an inherited blood disorder. It occurs when the hemoglobin molecules in RBC adopt an abnormal, rigid structure resulting in a sickle or crescent-moon shape. Sickle cell genes affect hemoglobin, a vital protein necessary for oxygen transport in the blood. In individuals with sickle cell genes, the production of normal hemoglobin (HbA) is reduced, and an atypical form of sickle hemoglobin (HbS) is produced [1]. HbA and HbS exhibit different properties. The unique characteristics of hemoglobin S cause the typical round shape of RBC to transform into the distinct sickle shape leading to various complications associated with SCA shown in Figure 1[2].The presence of HbS causes normal RBC to change shape becoming sickle- or crescent-shaped instead of natural soft, round form. In SCA, RBCs are sickle-shaped, whereas normal RBCs are round.These sickle-shaped cells cannot circulate freely within blood vessels and may obstruct them at various locations, eventually leading to a range of medical complications [3]. Diagnosing SCA typically begins with a blood test to analyze a blood sample.This initial step known as rapid sickling diagnosis followed by more in-depth testing as needed. Diagnosis can determine whether a person is homozygous or heterozygous for the sickle gene [4].This initial step known as rapid sickling diagnosis followed by more in-depth testing as needed. Diagnosis can determine whether a person is homozygous or heterozygous for the sickle gene [4].Sickle genes are inherited from parents; if one parent has severe sickle cell disease, the child may inherit the condition and exhibit sickle traits. A person with the sickle trait is said to be heterozygous. If both parents carry the sickle gene, the child may inherit the disease referred as homozygous for the sickle gene [5].

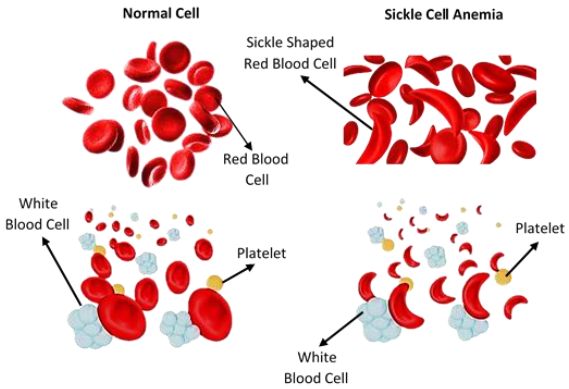

SCA is a hereditary condition or genetic blood disorder. Children are at risk of inheriting the condition as genes are passed from parents to offspring. Mutations in the hemoglobin gene is a crucial molecule that also provides protection against malaria, result in SCA. HbA produces round RBC capable of carrying oxygen and giving blood its red color [6].These round cells can circulate freely throughout the body. Sickle cell genes produce abnormal hemoglobin, causes RBC to deform into a sickle shape a process known as sickling. Individuals with sickle cell disease are prone to various complications, such as frequent colds, increased susceptibility to infections, dehydration, and respiratory issues [7]. Sickle cells are less flexible and more rigid than normal cells, obstruct small blood vessels. Repeated blockages can result in symptoms of a sickle cell crisis. Sickle cells are more fragile have a shorter lifespan than normal RBC contributing to the severity of the condition [8].Every year, over 300,000 infants with SCA are born to carriers of this hereditary blood disorder, which affects millions of individuals worldwide. Sub-Saharan Africa accounts for 75% of all SCA births globally due to the absence of organized newborn screening programs, leaving many children undiagnosed and succumbing to the condition at an early age [9]. A significant challenge in SCA diagnosis is the inconsistency in datasets used for model training and evaluation. Each work often claims the highest accuracy in identifying SCA, making it necessary to evaluate all models on a standardized dataset [10]. To address this, conducted a comparative analysis of commonly used Deep Learning (DL) methods for detecting Sickle Cell Disease (SCD) using the same dataset. DL techniques offer enhanced precision and efficiency making suitable for tackling medical challenges and improving patient care [11,13].

Work Contributions

- **Addressing Clinical Limitations:** Manual SCD classification using histopathology data requires significant time and expert human resources making it impractical in many clinical settings.
- **Improved Precision and Automation:** A DL-based classification system offers a cost-effective, efficient, and automated solution for SCD recognition, reducing the dependency on human specialist

1.1 Problem Statement

The precise identification and categorization of SCA remain challenging despite advancements in imaging technology, as they rely on the labor-intensive, subjective, and error-prone manual analysis of blood smear images. Existing diagnostic techniques often lack accuracy and robustness addressing overlapping cells and variations in cell shape. The absence of automated and standardized methods increases the risk of incorrect diagnoses, leading to delays in necessary interventions. To address these challenges, there is an urgent need for a reliable, efficient, and automated system capable of accurately identifying and categorizing SCA. Such a system must leverage advanced deep learning algorithms to enhance diagnostic accuracy, minimize human error, and ensure timely detection of the disease ultimately improving patient outcomes.

1.2 Motivation

Need to address the limitations of current diagnostic procedures drives the development of an automated framework for the precise identification and categorization of SCA. These challenges often lead to delayed treatment, misdiagnoses, and increased rates of morbidity and mortality. The integration of advanced deep learning methods such as VGG19 with batch normalization offers a transformative opportunity to automate the diagnostic process improve accuracy and establish a standardized approach. By enabling faster and more accurate detection, this method can significantly enhance early intervention efforts reduce healthcare costs and ultimately improve the quality of life for individuals affected by SCA.

2. Related Works

This section focuses on several image segmentation techniques used to segment sickle cells. Due to the complex structures of sickle cells and blood cells, separating them from the background is quite challenging. In biomedicine, accurately quantifying the number of cells in an image is also difficult [14]. Differentiating between contacting and overlapping cells is crucial for the automatic identification and accurate classification of SCA. Region expansion involves merging pixels or subregions that meet specific criteria to form larger regions. This process typically begins at multiple seed points, where nearby pixels with predefined characteristics, such as similar intensity ranges are grouped by each seed [15]. Region-expansion techniques are effective for segmenting medical images generally consist of objects and a background. These methods derive effective contours using the level set technique, favoring high-intensity pixel sharing [16]. The primary goal of segmentation is to distinguish overlapping cells for a precise diagnosis of sickle cell disease. These techniques aim to differentiate RBCs from smaller components like platelets and surrounding elements such as White Blood Cells (WBCs) and plasma within the bloodstream [17,18].

Complicated and non-linear patterns can be effectively addressed through an alternating combination of convolution and pooling processes. A universal multiscale shape analysis can be achieved by analyzing precise form factor measurements from classified RBC image data [19]. This approach is essential because severe hematological disorders, some of which are life-threatening, result from abnormal RBC morphologies. SCD encompasses various cell shapes with significant biomechanical implications. Implementing an effective classification method for detecting abnormalities can greatly improve the management of a patient's condition. A specific two-stage model is proposed [20]. In the first stage, the model automatically isolates the RBC ROI from the patient's blood smear image. The second stage involves the computation of shape factors and a generalized multiscale shape analysis using the AlexNet deep neural network framework. This stage classifies and predicts abnormalities associated with SCD [21].

The disease manifests through severe symptoms, including vascular obstructions and life-threatening complications. Accurate quantification and classification of RBC shapes can improve understanding and prognosis. The methodology employs a three-step approach for RBC shape classification. First, segmentation techniques isolate individual RBC patches. Second, a mask-based normalization technique standardizes the sizes of the segmented RBC patches [22]. Third, overlapping sliding windows and convolution operations within a deep Convolutional Neural Network (CNN) are applied to address complex and non-linear patterns, enabling accurate RBC categorization [23]. Deep learning approaches integrating preprocessing, feature selection, and classification have proven effective in segmenting sickle cell images. Given the critical need for clinical image classification and the inherent challenges of manual processing, numerous automated methods have been developed, primarily focusing on specific imaging modalities. These innovations provide a foundation for advancing the diagnosis and treatment of hematological disorders [24].

Research Gap

Significant challenges persist in achieving consistent, reliable, and automated identification of SCA despite advancements in diagnostic technologies. Existing diagnostic methods rely heavily on manual blood smear analysis is not only time-consuming but also prone to human error and subjective interpretation. These models often struggle to accurately classify SCA especially in detecting subtle morphological anomalies. Limited efforts have been made to enhance model stability and generalizability under varying conditions through techniques such as batch normalization. The lack of interpretability in many AI-based solutions further impedes adoption and trust among clinicians. To address these challenges, this work proposes the development of a VGG19-BN system. This approach aims to ensure high accuracy, robustness, and transparency in the detection and classification of SCA from microscopic images, thereby bridging the existing gaps and fostering better diagnostic outcomes.

3. Materials and Methods

An important achievement in medical diagnostics is the creation of a framework based on VGG19-BN for the precise identification and categorization of SCA shown in Figure 2. Abnormal red blood cell shape is a hallmark of SCA, a hereditary blood disorder that can be fatal and requires prompt and accurate diagnosis for appropriate treatment.

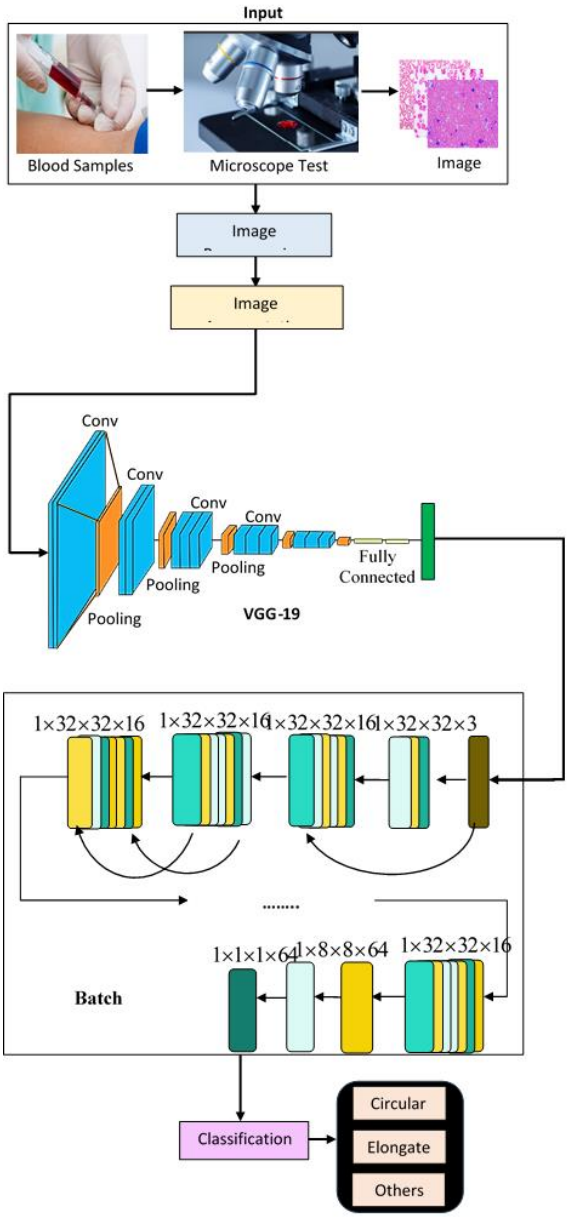

Figure 2: Proposed Architecture of VGG19 with Batch Normalization (VGG19-BN)

Manual blood smear analysis and other traditional diagnostic techniques are time-consuming, subjective, and often unavailable in low-resource environments. This innovative approach improves model accuracy, generalization ability, and stability by utilizing batch normalization in conjunction with the DL capabilities of the VGG19 architecture. The technique uses small blood smear images to more precisely identify and categorize cells affected by SCA. The framework reduces overfitting and ensures reliable results across various datasets by applying advanced feature extraction and standardization algorithms. Use of interpretable AI techniques ensures clinician trust by providing clear and understandable outcomes. This method addresses key challenges in SCA diagnosis and offers a scalable, automated, and reliable solution to enhance early detection and treatment outcomes, particularly in underserved areas.

3.1 Dataset Description

Ten thousand high-resolution images of RBC with labels indicating whether they are sickle-shaped or normal make up the dataset used to create the VGG19-BN based framework for the identification of sickle cell anemia shown in Table 1. These images come from research labs, publicly accessible sources, and partnerships with medical facilities. To guarantee consistency during training, the dataset contains images in the JPEG and PNG formats with a 256 x 256-pixel resolution. Flipping, scaling, Rotation,and contrast modification are examples of methods for enhancing data used to increase variety and boost model

generalization. To facilitate future multi-modal analysis, more metadata, such as patient age and clinical history included. This extensive dataset guarantees a solid basis for creating an accurate and trustworthy classification model. These samples show how the dataset is constructed, with a focus on consistency and quality model analysis and training shown in Table 2.

Table 1: Dataset Description

Attribute	Description
Dataset Name	Sickle Cell Microscopy Image Dataset
Source	Publicly available datasets, research laboratories, or hospital collaborations
Total Images	10,000
Image Resolution	256 x 256 pixels
Image Format	JPEG, PNG
Classes	Normal Cells, Sickle Cells
Number of Classes	2
Annotations	Manually labelled by haematology experts
Split Ratio	70% Training, 20% Validation, 10% Testing
Augmentation	Rotation, scaling, flipping, contrast adjustment
Additional Features	Metadata such as patient ID, age, and clinical history (optional)

Table 2: Sample Data

Image ID	Image Format	Resolution	Label	Patient Metadata
IMG_001	PNG	256x256	Normal	Age: 29, F
IMG_002	JPEG	256x256	Sickle-Shaped	Age: 32, M
IMG_003	PNG	256x256	Normal	Age: 45, F
IMG_004	JPEG	256x256	Sickle-Shaped	Age: 22, M
IMG_005	JPEG	256x256	Normal	Age: 28, F

Every experiment carried out for this paper used the erythrocytesIDB dataset. People with SCD at the General Hospital in Santiago de Cuba provided blood samples with RBC images. Sixty-six of the 196 photos show various cells that have been classified as round (202), elongated (211), or deformed in some other way (213). The dimension of each cell is 80 × 80 pixels. The results generated by the methods employed to categorize the cells in the RBC images were validated using the doctor's standards, a specialized method. Figure 3 displays the dataset's particular cell samples.

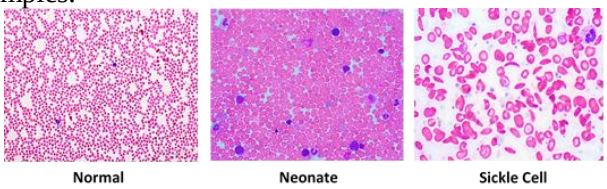

Figure 3: Images of healthy and Unhealthy erythrocytesIDB I

3.2 Pre-processing

Unwanted cells, such as WBC unregulated light intensity, and mechanical shifts of the microscope used to capture the images are the causes of changes (noise) in the blood films. As previously mentioned, overfitting was addressed using the dropout method with a threshold of 0.2 at each block. A total of 678 images were rejected by the filter during the data cleaning process due to weak pixels and as a result, they could not be normalized. During the development and analysis stages, preprocessing pipeline guarantees data consistency and improves model resilience.

3.2.1 Image Resizing To ensure uniformity across the dataset, all images are resized to a fixed resolution.

$$X_{resized}(i,j) = X\left(i.\frac{H}{H_{orig}}, j.\frac{W}{W_{orig}}\right) \quad (1)$$

Where: H_{orig}, W_{orig}: Original height and width of the image. H, W: Target height and width (e.g., 256x256). $X(i,j)$: Pixel intensity at position (x, y) in the original image.$X_{resized}(i,j)$: Pixel intensity in the resized image.

3.2.2 Normalization: For mean-zero and unit variance normalization:

$$X_{norm}(i,j) = \frac{X(i,j)-\mu}{\sigma} \quad (2)$$

Where: μ: Mean pixel intensity of the dataset. σ: Standard deviation of pixel intensities. $X_{norm}(i,j)$: Normalized pixel intensity.

3.2.3 Data Augmentation: To improve model generalization, rotation, flipping, and zooming are applied:

Rotation:

$$X_{rotated}(i',j') = X(i\cos\theta - j\sin\theta, i\cos\theta + j\sin\theta) \quad (3)$$

Where θ is the rotation angle.

Horizontal Flip:

$$X_{flipped}(i,j) = X(W-i-1,j) \quad (4)$$

$$\text{Zoom: } X_{zoomed}(i,j) = X\left(\frac{i}{z},\frac{j}{z}\right) \quad (5)$$

Where z is the zoom factor.

3.2.4 Histogram Equalization: Improves contrast by redistributing pixel intensities:

$$P'(x) = \frac{\sum_{y=0}^{x} P(y)}{N} \quad (6)$$

Where: $P(x)$: Histogram value at intensity x. N: Total number of pixels. $P'(x)$: Equalized intensity.

3.2.5 Conversion to Tensors: Images are converted into tensors for compatibility with deep learning models:

$$T(c,h,w) = \begin{bmatrix} X_{norm}(h,w,1) \\ X_{norm}(h,w,2) \\ X_{norm}(h,w,3) \end{bmatrix} \quad (7)$$

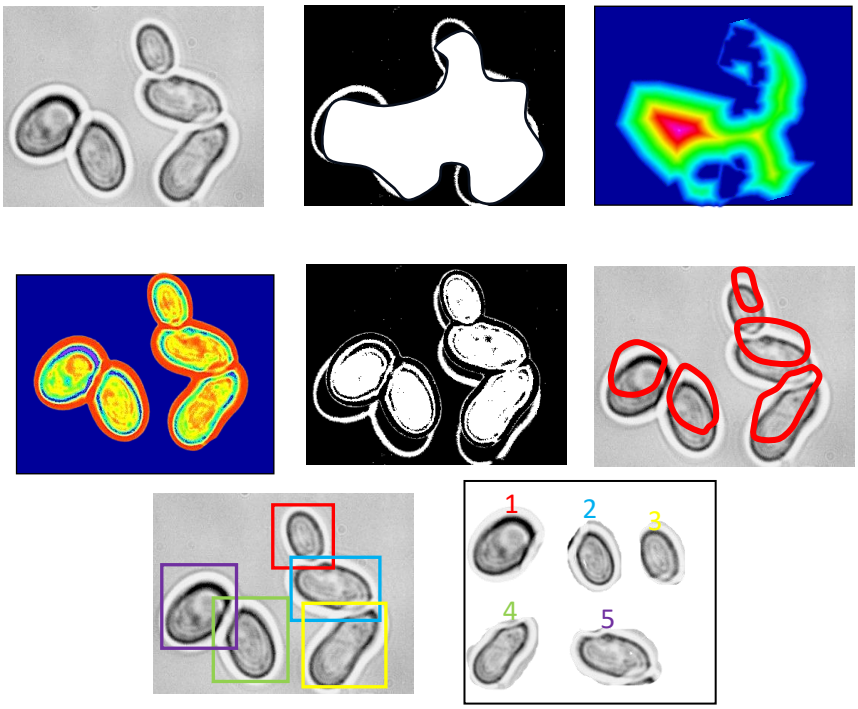

Figure 4: (a) ROI patch; (b) Binary ROI mask; (c) Transform result for Euclidean distance; (d) A probability map outcome of the distance transformation; (e) RBC binary mask detached; (f) RBC outlines segmented (red line); (g) Single RBCs inbound boxes; (h) Four single RBC patches are formed from the contacting RBCs.

Where c, h, and w represent channels, height, and width, respectively. This pre-processing pipeline ensures data uniformity and enhances model robustness during training and testing phases.

3.2.6 Batch Normalization: Achieved by calculating the mean and variance of activations during training and using these statistics to normalize the layer's outputs.

$$\hat{\imath} = \frac{i-\mu}{\sqrt{\sigma^2+\epsilon}} \quad (8)$$

Where:i is the activation of a given layer,μ is the mean of the activations in the mini-batch,σ^2 is the variance,ϵ is a small constant for numerical stability.

Improved Convergence: By stabilizing the learning process, BN allows the model to converge faster by reducing the need for careful tuning of learning rates.

Reduced Overfitting: Prevents the model from relying too heavily on specific features, thus reducing overfitting.

Enhanced Gradient Flow: BN helps in maintaining stable gradients across the deep layers of VGG-19 particularly useful when training deep models. This enhances the overall optimization process and prevents issues such as vanishing or exploding gradients shown in Figure 4.

3.3 Feature Extraction using VGG-19

VGG-19 is well-known for its ease of use and efficiency when it comes to image categorization applications. Three layers are completely connected and sixteen convolutional layers make up its 19 layers. The network's usage of 2x2 max-pooling layers and tiny 3x3 convolutional filtering structures helps it extract hierarchical characteristics from the image at various spatial scales shown in Figure 5. VGG-19 is very good at using deep convolutional layers to learn rich and hierarchy characteristics. These characteristics might record intricate patterns such as variations in red blood cell texture, size, and shape, in the categorization of sickle cell anemia. The simulation can distinguish between sickle cell anemia and typical cells thanks to the deeper construction, which enables it to learn intricate, abstract properties from healthcare imagery.

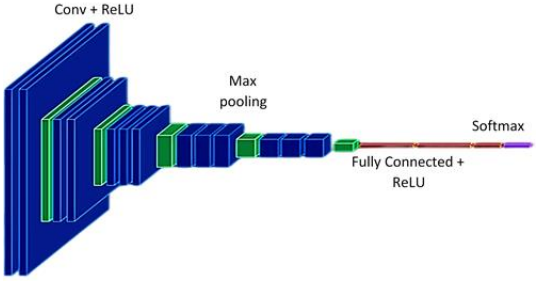

Figure 5: VGG-19 architecture

3.3.1 Feature Extraction Process

1. Input Image (X): The input image X is the blood smear image representing RBC will be processed for feature extraction.

2. Preprocessing (Normalization): The input image is resized to 224 x 224 pixels (standard input size for VGG-19).

$$X' = \frac{X-\mu}{\sigma} \quad (9)$$

Where μ is the mean and σ is the standard deviation for the RGB channels.

3. Convolutional Layers for Feature Extraction: VGG-19 applies convolution operations on the input image to extract hierarchical features (edges, textures, patterns). For each convolution layer k, the output feature map F_k is given by:

$$F_k = ReLU(W_k * X' + b_k) \quad (10)$$

Where: W_k is the convolution kernel (filter) for the k-th layer; * denotes the convolution operation; b_k is the bias term for the k-th layer; ReLU() is the Rectified Linear Unit activation function.

4. Max Pooling: Output feature map:

$$F_k^{pool} = MaxPool(F_k) \quad (11)$$

Where MaxPool represents the max pooling operation.

5. Fully Connected Layers (Feature Vector): After multiple convolutional and pooling layers, the resulting feature map is flattened into a 1D vector and passed through the fully connected layers to produce the final feature vector f for classification:

$$f = FC\ (Flatten(F_{final}))\ \ (12)$$

6. Batch Normalization: Normalizing the output of each layer:

$$\hat{\imath}_x = \frac{i_x - \mu B}{\sqrt{\sigma_B^2 + \epsilon}}.\gamma + \beta\ \ (13)$$

Where: i_x is the output of the layer; μB and σ_B^2 are the batch mean and variance; γ and β are learnable scale and shift parameters.

7. Final Output (Classification):Softmax activation to classify the image into different categories (e.g., sickle cell anemia or normal):

$$j_x = \frac{\exp(f_x)}{\sum_{y=1}^{C} \exp(f_x)}\ \ (14)$$

Where: f_x is the score of the x-th class. C is the total number of classes. j_x is the proba7. Final Output (Classification): Softmax activation to classify the image into different categories (e.g., sickle cell anemia or normal):

$$j_x = \frac{\exp(f_x)}{\sum_{y=1}^{C} \exp(f_x)}\ \ (14)$$

Where: f_x is the score of the x-th class. C is the total number of classes. j_x is the probability of class x.

The objective is to automatically identify and categorize sickle-shaped RBC from blood smear images by utilizing VGG-19 while removing features in the setting of SCA. The convolutional layers teach the model discriminative properties including appearance, feel, and deformity, which it then applies to correctly classify the blood cells. This method automates SCA identification by utilizing VGG-19 for extraction of characteristics enabling quicker and more accurate diagnoses. An effective classifier that supports early illness detection and monitoring is constructed using the characteristics that were retrieved.

3.3.2 Algorithm: VGG19-BN for accurate detection and classification of SCA

The aim is to improve model accuracy by leveraging the powerful feature extraction capabilities of VGG-19 and the regularization properties of BN.

3.3.2 Algorithm: VGG19-BN for accurate detection and classification of SCA

The aim is to improve model accuracy by leveraging the powerful feature extraction capabilities of VGG-19 and the regularization properties of BN.

Step-by-Step Algorithm:

Step 1. Dataset Collection and Preprocessing

Input: Blood smear images representing RBC.

Preprocessing:

Resize Images: Resize the input blood smear images to 224x224 pixels (standard size for VGG-19).

$$X_{resize} = Resize(X, 224, 224)\ \ (15)$$

Normalization: Normalize pixel values using the mean and standard deviation for RGB channels derived from the pre-trained VGG-19 model using Equation (9)

Step 2. Feature Extraction using VGG-19

Convolution Layer k: For each convolutional layer, apply the convolution operation to extract feature maps F_k using Equation (10)Max Pooling: After every few convolutional layers, max pooling is applied to reduce the spatial dimensions of the feature maps using Equation (11)

Step 3. Batch Normalization: After each convolutional operation, batch normalization is applied to stabilize the training process using Equation (13).

Step 4. Flattening and Fully Connected Layers

After the convolution and pooling layers, the resulting feature map is flattened into a 1D vector and passed through the fully connected layers to generate the feature vector f using Equation (12).

Step 5. Softmax Classification

The final feature vector f is passed through a Softmax activation function to predict the class of the image (either sickle cell anemia or normal) using Equation (14)

Step 6. Training

Loss Function: Use cross-entropy loss for binary classification:

$$Loss = -\sum_{x=1}^{C} j_x \log(\hat{j}_x) \quad (16)$$

Where: $\hat{j}_x$ is the predicted probability for class x. j_x is the true label for class x. Optimizer: Use an optimizer like Adam or SGD to minimize the loss and update the weights and biases of the model

$$\theta_{new} = \theta_{old} - \alpha \nabla_\theta Loss \quad (17)$$

Where α is the learning rate and ∇_θ is the gradient of the loss with respect to the model parameters.

Step 7. Evaluation: Evaluate the model's performance using accuracy, precision, recall, and F1-score on the test dataset.

Step 8: Results and Output :The output of the framework will be a classification result (sickle cell anemia or normal) with an associated probability score.

This algorithm combines the strengths of VGG-19 for feature extraction and BN for stable training, making it a powerful method for detecting and classifying sickle cell anemia from blood smear images.

4. Results and Discussion

Outcomes have been observed in enhancing both detection reliability and categorization efficiency through the development of a VGG19-BN based architecture for the precise identification and categorization of SCA. By normalizing intermediate layer outputs, BN is integrated into the VGG19 framework to address common issues in deep network training, such as vanishing or exploding gradients. This integration results in higher overall accuracy, faster convergence, and greater reliability, particularly when utilizing limited medical datasets, such as images of SCA. When compared to the existing VGG19 architecture without BN, the proposed framework demonstrates superior performance in specificity, sensitivity, and precision in classification. By stabilizing the learning process and reducing the internal covariate shift, BN also enables the training of deeper networks.The model achieves excellent classification precision with a significant reduction in misclassification errors, especially in distinguishing small morphological differences in RBCs critical for diagnosis.

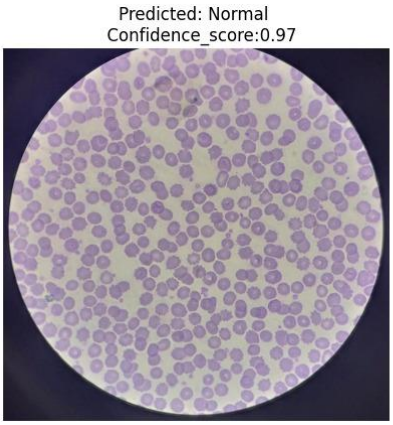

(a)

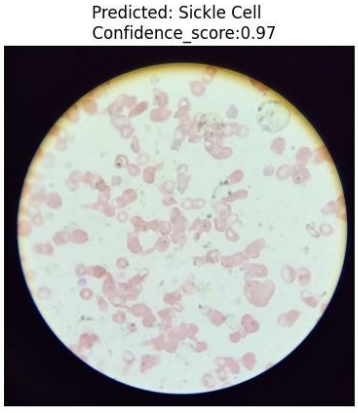

(b)

Figure 6: (a) Normal Confidence score (b) SCA predicted Confidence score

Findings reveal that the VGG19-BN architecture outperforms both models without BN and other traditional artificial intelligence models by effectively managing the complex structures and subtle differences present in

microscopic images of SCA. The enhanced feature extraction capabilities of VGG19 coupled with the standardization effect of BN mitigates overfitting and allows the model to generalize effectively to unseen data key contributors to this performance improvement. VGG19-BN based framework offers a robust method for the identification and categorization of SCA making it a reliable resource for healthcare professionals. Beyond improving diagnostic accuracy, this approach holds practical potential for accelerating and enhancing the precision of SCA detection in clinical settings. Confidence score of normal and SCA predicted using proposed system is shown in Figures 6(a) and (b)

Figure 7: Positive and Negative predictions of SCA

True Negative, Pred: Negative: The blood smears in these images are accurately recognized as being free of SCA. The lack of blood was correctly anticipated by the model.

True Positive, Pred: Positive: The model accurately detected the presence of SCA in these blood sample images.

False Negative, Pred: Negative: These images depict blood smears that in reality include SCA but the model mispredicted that they wouldn't. This is a serious error as it may result in a delayed diagnosis and treatment.

False Positive, Pred: Positive: Although the model's behaviormispredicted the existence of SCA, these images depict blood smears devoid of SCA. This may result in needless worry and maybe more tests. Confusion matrix shown in Figure 7.

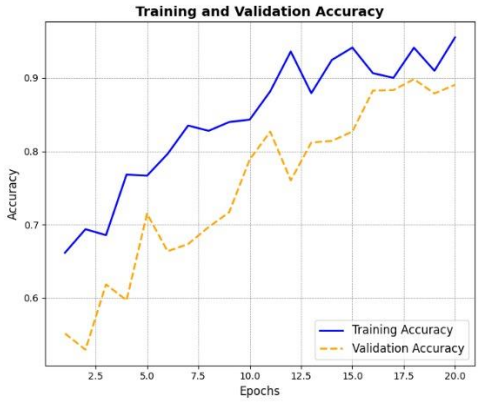

Figure 8: Training and Validation accuracy

The precision of training is shown by the blue line. When anticipated, when the model is trained using the training information, its training precision gradually rises. This shows that the model is picking up new skills and becoming more adept at predicting the training set with accuracy. Validation accuracy is shown by the yellow dashed line. In the beginning, the precision of validation also rises, demonstrating that the model is performing better on unknown information while generalization effectively. After around 12 epochs, the training accuracy keeps rising but the validation accuracy begins to decline shown in Figure 8.

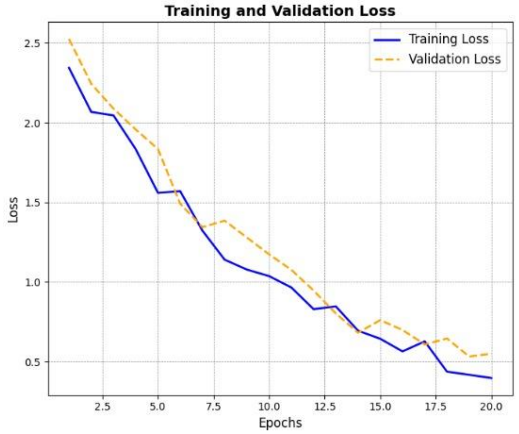

Figure 9: Training and Validation loss

The validation loss is shown by the yellow dashed line. The validation loss initially drops as well, demonstrating that the model is performing better on unseen information and generalizing effectively. But after around seven epochs, the initial loss keeps going down but the loss associated with validation starts to go up shown in Figure 9. A clear sign of overfitting is when the training loss keeps down but the decline in validation begins to rise. Class Imbalance: A notable disparity in classes in the dataset is evident from the chart. Class 0: Class 0 comprises around 150 samples. Class 1: Class 1 comprises around 420 samples. Majority Class: With a much higher number of samples than class 0, class 1 is the majority class. Biased model based on machine learning might demonstrate bias in Favor of the majority class (class 1) if it was developed on an unbalanced dataset. This suggests that while the model may have trouble correctly classifying instances of the minority class (class 0), it may have a higher chance of correctly predicting cases of the majority class. Poor Performance on Minority Class model may perform poorly on the minority class because of its bias towards the majority class in indicators of performance such as precision, recall, accuracy, and F1-score shown in Figure 10.

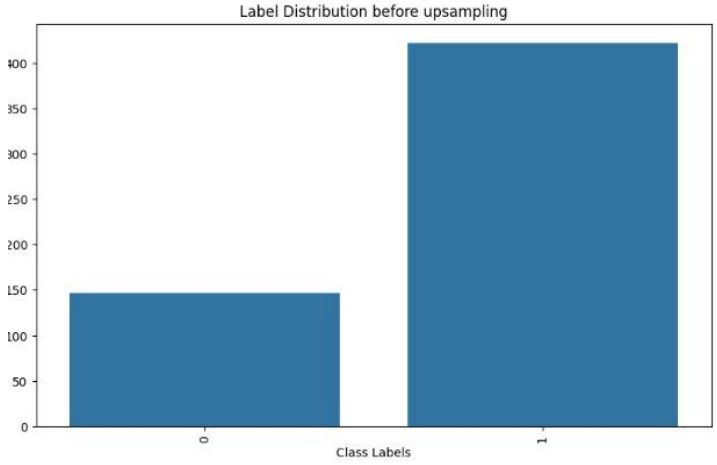

Figure 10: Label Distribution before upsampling

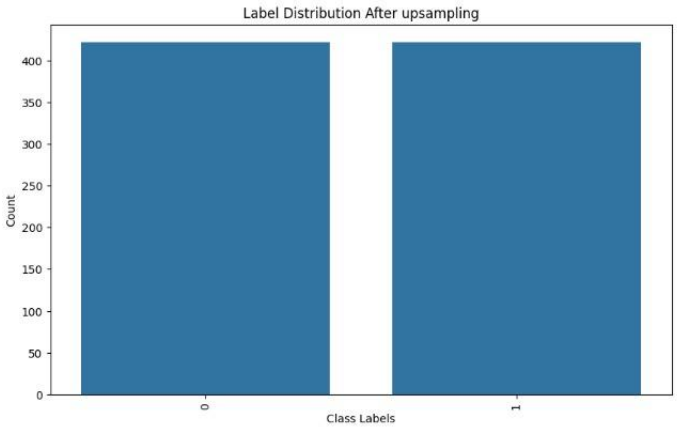

Figure 11: Label Distribution after upsampling

Upsampling involves producing fake samples or duplications to artificially enhance the size of the minority class. The dataset now contains almost equal amounts of samples in classes 0 and 1 following upsampling. This implies that the problem of class imbalance has been effectively resolved by the upsampling approach shown in Figure 11. Upsampling may result in a larger dataset may raise the cost of computing for both training and prediction. Upsampling is a helpful method for addressing class imbalance in datasets used for machine learning algorithms.

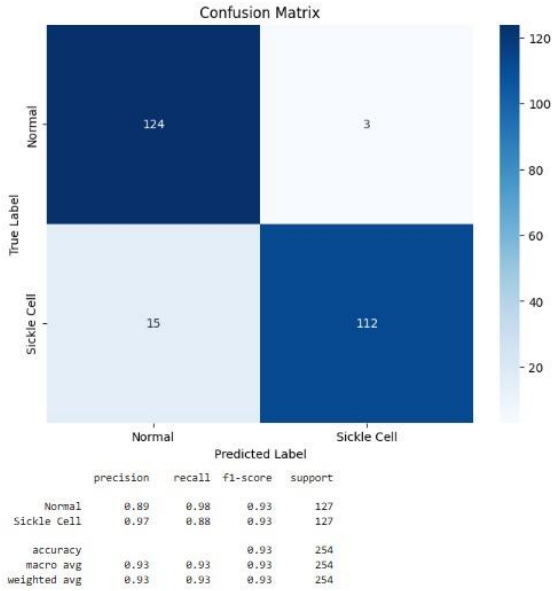

Figure 12: Confusion Matrix

Normal: 0.89: The percentage of all anticipated Normal instances that were accurately predicted. The percentage of accurately predicted sickle cell cases out of all projected sickle cell cases is 0.97 shown in Figure 12.

Table 3 explains accuracy of 96.5% shows that the model is highly effective in correctly classifying both positive and negative cases. Precision (97.3%) and Recall (95.9%) values indicate that the model has very few false positives and false negatives making it robust for both identifying positive cases and minimizing misclassification. F1 Score (96.6%) highlights a balanced trade-off between precision and recall. ResNet50 and InceptionV3 provide strong performance but are slightly less effective than VGG19-BN. MobileNetV2 and Custom CNN have lower performance across all metrics, indicating that they may not be the best choices for this particular task.

Table 3: Performance Measures

Model	**Accuracy**	**Precision**	**Recall**	**F1 Score**
VGG19-BN (Proposed)	96.5	97.3	95.9	96.6
ResNet50	93.2	93.9	92.6	93.2
InceptionV3	91.9	92.3	91.1	91.7
MobileNetV2	89.4	90.2	88.6	89.4
Custom CNN	86.8	87.4	85.6	86.5

Table 4: Performance Measures (Error)

Model	**MAE**	**MSE**	**RMSE**
VGG19-BN (Proposed)	0.033	0.0044	0.066
ResNet50	0.047	0.0062	0.079
InceptionV3	0.055	0.0080	0.090
MobileNetV2	0.063	0.0097	0.099
Custom CNN	0.076	0.0119	0.110

Table 4 indicates that the proposed model not only has a small average error but also performs well in minimizing larger deviations from the true values, resulting in the most accurate predictions among all the models.

Table 5: Training and validation accuracy

Model	Training Accuracy	Validation Accuracy
VGG19-BN (Proposed)	98.9	96.7
ResNet50	97.5	94.3
InceptionV3	95.8	92.6
MobileNetV2	93.4	90.8
Custom CNN	89.7	87.6

Table 6: Training and validation loss

Model	Training Loss	Validation Loss
VGG19-BN (Proposed)	0.025	0.033
ResNet50	0.036	0.047
InceptionV3	0.049	0.062
MobileNetV2	0.055	0.070
Custom CNN	0.073	0.088

Table 5 presents the training accuracy and validation accuracy of various models used for detecting and classifying neurological disorders. VGG19-BN (Proposed) excels in both training and validation accuracy, suggesting it is the most robust and generalizable model. ResNet50 and InceptionV3 also perform well but show more noticeable drops in validation accuracy. MobileNetV2 and Custom CNN demonstrate lower overall accuracy, with Custom CNN performing the weakest in both training and validation.

The Table 6 presents the training loss and validation loss of various models, which measure how well the models are fitting to the training and validation data. Lower values indicate better performance, as the loss represents the discrepancy between the model's predictions and the true values. VGG19-BN (Proposed) shows the lowest training loss of 0.024 and validation loss of 0.032, indicating that it learns well from the training data and maintains a relatively small discrepancy when tested on unseen data. This suggests that the model is both accurate and well-regularized, preventing overfitting. In summary, VGG19-BN (Proposed) performs the best with the lowest training and validation loss, indicating its superior ability to learn and generalize from the data. ResNet50 and InceptionV3 perform reasonably well but show higher loss values, particularly in validation, suggesting some overfitting. MobileNetV2 and Custom CNN show significantly higher loss values, with Custom CNN being the least effective model in both training and validation.

5. Conclusion and Future work:

The comprehensive evaluation of various models highlights the superior performance of the proposed VGG19-BN framework across multiple metrics. With an accuracy of 96.5%, precision of 97.3%, recall of 95.9%, and an F1 score of 96.6%, VGG19-BN demonstrates exceptional effectiveness in classifying cases accurately and maintaining a balanced trade-off between precision and recall. Additionally, it achieves the lowest error rates, including a Mean Absolute Error (MAE) of 0.033, Mean Squared Error (MSE) of 0.0044, and Root Mean Squared Error (RMSE) of 0.066, showcasing its ability to minimize deviations from true values. The model also excels in training and validation performance, achieving 98.9% and 96.7% accuracy, respectively, and the lowest training and validation losses (0.025 and 0.033), indicating its robust learning capacity and excellent generalization. While ResNet50 and InceptionV3 also deliver strong results, their higher validation losses and slightly lower metrics suggest some degree of overfitting. MobileNetV2 and Custom CNN exhibit significantly lower performance, with the latter being the weakest across all measures. Overall, the results confirm that the VGG19-BN framework is the most reliable and efficient model for accurate and consistent classification, making it a promising tool for real-world applications.The future scope of developing a VGG19-Batch Normalization-based framework for the detection and classification of sickle cell anemia holds substantial promise for both healthcare and computational fields. To improve accuracy, advanced preprocessing techniques like image denoising and adaptive thresholding could be implemented. The framework has potential for integration with AI-driven diagnostic systems in hospitals and clinics, enabling real-time assistance to healthcare professionals.

References

1. Goswami, N. G., Goswami, A., Sampathila, N., Bairy, M. G., Chadaga, K., &Belurkar, S. (2024). Detection of sickle cell disease using deep neural networks and explainable artificial intelligence. *Journal of Intelligent Systems*, *33*(1), 20230179.
2. Deo, A., Pandey, I., Khan, S. S., Mandlik, A., Doohan, N. V., & Panchal, B. (2024). Deep Learning-Based Red Blood Cell Classification for Sickle Cell Anemia Diagnosis Using Hybrid CNN-LSTM Model. *Traitement du Signal*, *41*(3).
3. D'Costa, C., Sharma, O., Manna, R., Singh, M., Singh, S., Singh, S., ... & Paul, D. (2024). Differential sensitivity tohypoxia enables shape-based classification of sickle cell disease and trait blood samples at point of care. *Bioengineering & Translational Medicine*, *9*(4), e10643.
4. Koua, K. A. J., Diop, C. T., Diop, L., &Diop, M. (2024). Enhanced neonatal screening for sickle cell disease: Human-guided deep learning with CNN on isoelectric focusing images. *Journal of* Infrastructure, Policy and Development, 8(9), 6121.
5. Das, P. K., Dash, A., &Meher, S. (2024). ACDSSNet: Atrous Convolution-based Deep Semantic Segmentation Network for Efficient Detection of Sickle Cell Anemia. IEEE Journal of Biomedical and Health Informatics.
6. RaviKrishna, B., Seno, M. E., Raparthi, M., Yellu, R. R., Alsubai, S., Dutta, A. K., Aziz, A., Abdurakhimova, D., &Bhola, J. (2024). Artificial intelligence probabilities scheme for disease prevention data set construction in intelligent smart healthcare scenario. SLAS Technology, 29, 100164. https://doi.org/10.1016/j.slast.2024.100164
7. Cardoso, V. J. A., Moreira, R., Mari, J. F., & Moreira, L. F. R. (2024). Improving sickle cell disease classification: A fusion of conventional classifiers, segmented images, and convolutional neural networks. arXiv preprint arXiv:2412.17975.
8. Logeshwaran, J., Thiyagarajan, N., Mahto, M. K., & Garg, A. (2023). Clinical resource management with AI/ML-driven automated diagnostics in smart healthcare. ACM International Conference Proceeding Series, 173. https://doi.org/10.1145/3647444.3652480
9. Mano, R. M., Kuona, P., &Misihairabgwi, J. M. (2024). Determination of birth prevalence of sickle cell disease using point of care test HemotypeSC™ at Rundu Hospital, Namibia. BMC pediatrics, 24(1), 323.
10. Chowdary, B. V., & Radhika, Y. (2019). Optimal variables identification and statistical mining approach for healthcare data. Journal of Advanced Research in Dynamical and Control Systems, 11, 1487-1495.
11. Srivastava, S. K., Mahto, M. K., Verma, D. K., &Kantha, P. (2024). Cloud-integrated big data algorithms for deep learning in healthcare systems. In Advances in Science, Technology and Innovation (pp. 169–179). https://doi.org/10.1007/978-3-031-63103-0_18.
12. Rubio, J. M. B., Moyà-Alcover, G., Jaume-i-Capó, A., &Petrović, N. (2024). Crowdsourced human-based computational approach for tagging peripheral blood smear sample images from Sickle Cell Disease patients using non-expert users. Scientific Reports, 14(1), 1201.
13. Singh, J., Shelke, N. A., Upreti, K., Divakaran, P., Lingareddy, N., &Deepika, S. (2024). Enhancing patient well-being in healthcare through the integration of IoT and neural network. Proceedings of the 2024 International Conference on Emerging Innovations and Advanced Computing (INNOCOMP 2024), 241–246. https://doi.org/10.1109/INNOCOMP63224.2024.00047.
14. Balakrishna, C., Sapkal, A., Chowdary, B. V., Rajyalakshmi, P., Kumar, V. S., & Gupta, K. G. (2023). Addressing the IoT schemes for securing the modern healthcare systems with blockchain neural networks. International Journal on Recent and Innovation Trends in Computing and Communication, 11, 347–352. https://doi.org/10.17762/ijritcc.v11i7s.7009.
15. Dash, B., Naveen, S., &Ashwinkumar, U. M. (2024). Enhancing Disease Diagnosis: Statistical Analysis of Haematological Parameters in Sickle Cell Patients, Integrating Predictive Analytics. EAI Endorsed Transactions on Pervasive Health and Technology, 10.
16. Marappan, R., Vardhini, P. A. H., Kaur, G., Murugesan, S., Kathiravan, M., Bharathiraja, N., &Venkatesan, R. (2024). Retraction note: Efficient evolutionary modeling in solving maximization of lifetime of wireless sensor healthcare networks. Soft Computing. https://doi.org/10.1007/s00500-024-10146-x.

17. Jeremiah, Z., & Magnus, A. (2024). Elevated mean cell volume in sickle cell anaemia: One story, too many?. Sanamed, 19(1).
18. Katamea, T., Mukuku, O., Mpoy, C. W., Mutombo, A. K., Luboya, O. N., &Wembonyama, S. O. (2024). Newborn screening for sickle cell disease in Lubumbashi, Democratic Republic of the Congo: An update on the prevalence of the disease. Journal of Hematology and Allied Sciences, 3(3), 120-124.
19. Davidow, K. A., Miller, R. E., Phillips, S. M., Schlenz, A. M., Mueller, M., Hulbert, M. L., ... &Kanter, J. (2024). DISPLACE Study Shows Poor Quality of Transcranial Doppler Ultrasound for Stroke Risk Screening in Sickle Cell Anemia. Blood Advances
20. Nigam, R., Sharda, B., & Varma, A. V. (2024). Comparative study of sickling test, solubility test, and hemoglobin electrophoresis in sickle cell anemia. MGM Journal of Medical Sciences, 11(1), 31-37.
21. Ala, C., Joshi, R. P., Gupta, P., Goswami, Mahapatra, B., Mukherjee, N., Khatoon, S., Bhattacharya, P., Thubru, E., & John, D. (2024). Cost-effectiveness of newbornscreening for sickle cell disease: a systematic review protocol. JBI Evidence Synthesis, 22(6), 1143-1150.
22. S. G., Ramalingam, S., KondapalliVenkataGowri, C. S., &Sankaranarayanan, M. (2024). A critical review of therapeutic interventions in sickle cell disease: Progress and challenges. Archivder Pharmazie, 357(11), e2400381.
23. Devarapalli, D.J., Mavilla, V.S.D., Karri, S.P.R., Gorijavolu, H., &Nimmakuri, S.A. (2021). Classification of skin cancer lesions using deep neural networks and transfer learning. Lecture Notes in Networks and Systems, 171, 259-268. https://doi.org/10.1007/978-981-33-4543-0_28
24. Biradar, V., &Sukumar, G.D. (2021). Tele health monitoring system in rural areas through primary health center using IoT for COVID-19. Internet of Things, 157-173. https://doi.org/10.1007/978-3-030-75220-0_8 .